

# INFLUENCE OF THE ELECTROCHEMICAL ENVIRONMENT ON DIFFUSION PROCESSES NEAR STEP AND ISLAND EDGES: Ag(111) and Ag(100)

Michael I. Haftel\* + and T. L. Einstein +

\*Code 6331, Naval Research Laboratory, Washington, DC. 20375-5343

+Department of Physics, University of Maryland, College Park, MD 20742-4111

## ABSTRACT

The electrochemical cell provides a potentially powerful means of altering morphology and islanding phenomena on metallic surfaces. Diffusion and attachment processes on terraces and near step and island edges are known to profoundly affect island sizes, shapes and coarsening kinetics. Using the surface-embedded-atom-model (SEAM) for describing metallic surfaces in the electrolytic environment, we calculate the dependence of the activation energies for the aforementioned diffusion processes on the deposited surface charge for the Ag(111) and Ag(100) surfaces in an electrolytic environment. While all these processes show some degree of dependence on the potential, the step-edge barrier and the edge diffusion processes are the most sensitive. Step-edge barriers increase (to over 1 eV) with large positive potential (0.85 V), while edge diffusion barriers monotonically decrease with positive surface charge on Ag(100) and Ag(111). We assess the effect these diffusion barriers have on island size/shapes and coarsening dynamics and discuss the implications on electrochemical tuning of islanding phenomena.

## INTRODUCTION

Several recent investigations [1-4] have indicated that the early film growth and morphology of metal surfaces can be radically different in the electrochemical cell than in ultra-high vacuum (UHV). Moreover, these surface features can change over rather small changes in the applied electrochemical potential, as exhibited in the needle-like growth of Ni on Au(111) [2] and the low-index reconstructions of Pt(110) [3], Au(100) and Au(111) [4]. In light of the intense interest in controlling and manipulating islanding phenomena, such as in the fabrication of self-assembled quantum dots [5], the possibility of exploiting the electrochemical environment, e.g., through the applied potential, to control these features naturally presents itself.

Island and step morphology depend a great deal on kinetic as well as thermodynamic factors. Both types of properties can often be predicted from atomic-level calculations. A huge body of work exists on the atomistic prediction of surface energetics and kinetics in the UHV environment, but virtually nothing for the electrochemical environment. The main difference in the electrochemical cell from UHV is the presence of a charged electrolytic double layer. While a few first-principles calculations exist [6,7] treating a vacuum double layer, calculations with large surface unit cells in electrolytic surroundings by first principles methods is still out of reach. The main purpose of this paper is to apply an atomistic approach, based on the embedded atom method (EAM) [8], taking into account the electrolytic double layer, to the investigation of the effect of the electrochemical potential on diffusion barriers at and near island- or step-edges, and further how changes in these barriers can influence the sizes, shapes, and diffusion of the islands themselves. We concentrate on the Ag(111) and Ag(100) surfaces since many experimental [9-12] and theoretical [13-14] studies on these surfaces have been carried out. Furthermore, the surface-embedded-atom-method (SEAM) [15,16] has proven to be reasonably accurate in predicting surface energetics for silver in UHV. We outline the SEAM approach in the next section. The following section assesses the influence of the electrolytic surface charge on kinetic barriers and then on the islanding phenomena themselves.

## EMBEDDED ATOM MODEL OF METAL-ELECTROLYTE INTERFACE

The SEAM approach to modeling the electrolytic double layer has been described previously [17]. The main modification of the usual EAM is that instead of describing the background electron density  $\rho_i$  at an atomic site  $i$  as a superposition of atomic electron densities  $\phi$  produced by all other atoms, this superposition is augmented by an amount  $\Delta\rho_i$  coming from the charge deposited on the metal surface by the electrolytic double layer, i.e.,

$$\rho_i = \sum_{j \neq i} \phi_j(r_{ij}) + \Delta\rho_i. \quad (1)$$

To convert a surface charge density  $\sigma$  to a volume electron density  $\Delta\rho$ , we introduce a height  $h$  over which this excess charge is uniformly distributed. Thus the excess effective electron density is

$$\Delta\rho_i = -\sigma / h = -q / Ah, \quad (2)$$

where  $q$  is the total charge,  $A$  the surface area, with the excess applying only to surface atoms.

Another parameter,  $b$  – a linear coefficient of  $\rho$  in the embedding function  $F(\rho)$  – must be determined [17]. This term has no effect on charge-neutral systems, but comes into play when surface charge is present. Together,  $h$  and  $b$  are the two free parameters of our model. Once these parameters are determined one can calculate the total energy  $E$  of the system, the potential  $\Phi$  as a function of charge  $\Phi(q) = \partial E / \partial q$ , and the differential capacitance  $1/C = \partial \Phi(q) / \partial q$ . As in [17]  $h$  is determined by the (Helmholtz) capacitance of Ag(111) at high electrolytic concentration in aqueous solution ( $\sim 75 \mu\text{F}/\text{cm}^2$ ). Unlike in ref. [17] we fit the  $b$  parameter to the (111) work function of  $e\Phi(0) = 4.4 \text{ eV}$ . This leads to  $h = 1.38 \text{ \AA}$ ,  $b = 31.76 \text{ eV \AA}^3$ . The  $h$  value is close to the effective height of the dipole layer for Ag of  $1.2 \text{ \AA}$  calculated by Schmickler [18] with LDA in a jellium model. A similar fitting procedure was also carried out for Au. For both metals, once  $h$  and  $b$  are fit to (111) properties [19], the relative positions of the potential of zero charge (PZC) for the other low-index faces are in reasonable agreement with experiment [20]. Although water is not treated at the atomic level in our approach, its main effect – providing a dielectric medium with a high dielectric constant – is approximated by neglecting a contribution to the total energy, or to the capacitance [17], coming from the double layer acting like a static parallel plate capacitor. This term would be important for vacuum double layers or at low ionic concentrations.

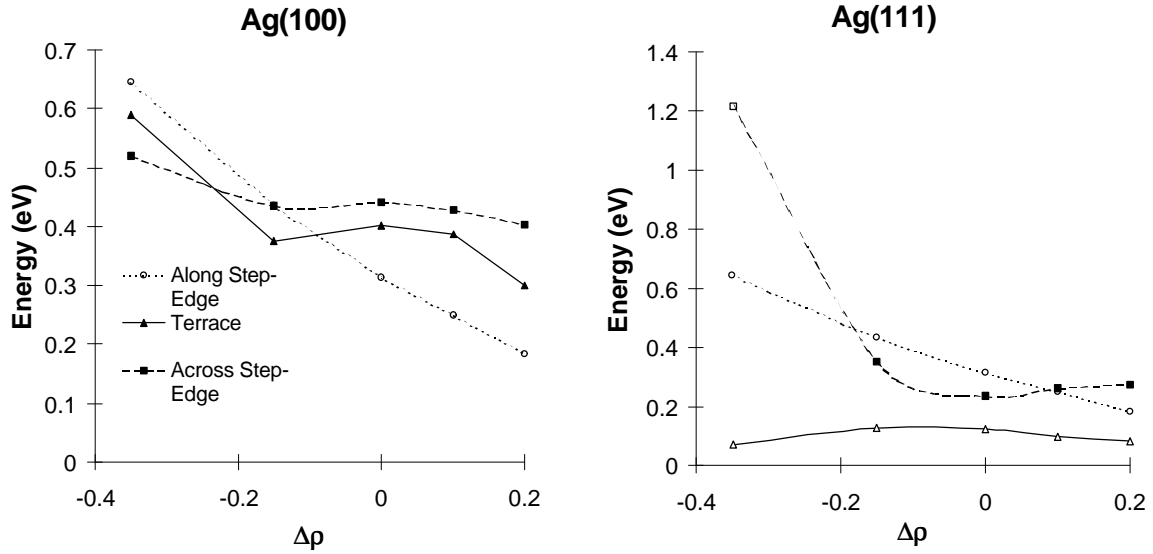
## RESULTS

Table I gives the correspondence between the potential  $\Phi(q)$  and the electron density shift  $\Delta\rho$  for Ag(100) and Ag(111). This potential is the potential across the double layer, which is unmeasurable. However, *changes* in this potential correspond to the same *changes* in the potential across the electrochemical cell. For this reason we also include the change in potential  $\Delta\Phi(q) = \Phi(q) - \Phi(0)$  as this corresponds to the difference between the actual potential and the potential-of-zero-charge (PZC). We also include the charge-variation of surface stress,  $f = (\partial E / \partial A)_q$ , where  $A$  is the surface area.

**Table I**

**The relative double layer potential  $\Delta\Phi$ , relative to that of Ag(111) at zero charge (4.378 V), and surface stress  $f$  as functions of the effective excess electron density.  $\rho_0$  is the equilibrium bulk electron density.**

$\Delta\rho/\rho_0$		-0.35	-0.15	0.0	0.10	0.20
Ag(100)						
$\Delta\Phi(q)$	(V)	0.701	0.231	-0.051	-0.216	-0.655
$f$	(meV/ $\text{\AA}^2$ )	175	166	159	152	105
Ag(111)						
$\Delta\Phi(q)$	(V)	0.854	0.324	0.0	-0.543	-1.108
$f$	(meV/ $\text{\AA}^2$ )	146	178	200	158	98



**Figure 1: Activation barriers for terrace diffusion, and diffusion along and over the step-edge, on Ag(100) and Ag(111). The filled markers indicate that exchange diffusion is preferable. For Ag(111) results are for the A step-edge, i.e., with (100) microfacets. The curves are guides to the eye.**

We have calculated the diffusion barriers on the open terrace, across step edges, along step edges, and around corners and kinks, as well as attachment and detachment barriers at step edges and kinks. Figure 1 illustrates the dependence of terrace diffusion barriers, step-edge barriers, and edge diffusion barriers on the surface charge. For brevity, here and below,  $\rho_0$ , the bulk electron density, is taken to be implicitly 1.0, i.e.,  $\Delta\rho$  is shorthand for  $\Delta\rho/\rho_0$ .

Large sensitivities to surface charge occur for most of the diffusion constants. Generally, diffusion barriers rise with increasing positive charge or voltage. Trends are not necessarily the same for (111) as (100) (e.g., the terrace diffusion barriers), and often the preferred diffusion mechanism, hopping or exchange, may change with surface charge. The Ehrlich-Schwobel barrier  $E_{es}$ , the difference between the upper step-edge and the terrace diffusion barriers, exhibits opposite trends for (100) and (111), being very large at high positive charge ( $\Delta\rho = -35\%$ ) for (111) and even becoming negative under the same conditions on (100). The variations in Fig. 1 suggest the possibility of electrochemical “tuning” of diffusion barriers, important in 3D and 2D islanding phenomena.

The trends exhibited in Fig. 1 are the result of two influences of the surface charge. As the surface environment become more electron-starved, the price of bond-breaking increases, i.e., the work function increases. Thus bond-breaking becomes more costly with positive surface charge leading to larger diffusion barriers. The bond-breaking argument, however, ignores relaxation effects, which are linked to the tensile stress and strain of the surface. For the open terrace we find that higher tensile stress tends to increase hopping barriers and decrease exchange barriers, a trend fully consistent with that pointed out by Yu and Scheffler [21] in first-principles calculations. We also find a similar trend for the exchange barrier over the step-edge (more stress  $\rightarrow$  smaller barriers). The bond-breaking charge effect shows up most dramatically in the very large step-edge barrier for Ag(111) for  $\Delta\rho = -35\%$ , while the terrace diffusion barriers on the same surface correlate rather well with the stress effect. Diffusion along the step-edge, for both surfaces, appears to be primarily influenced by the bond-breaking effect. The nonmonotonic nature of many of the calculated diffusion barriers can be traced to the opposite influences of the bond saturation and surface stress, as well as to changes in the preferred mechanism, hopping or exchange.

How can the variation of diffusion barriers influence the size and shapes of 2D islands? We utilize the nucleation theory results [22] for the average island size (in number of atoms)  $\langle N \rangle$

$$\langle N \rangle = (D\theta^2 / 3Fa^4)^{1/3}, \quad (3)$$

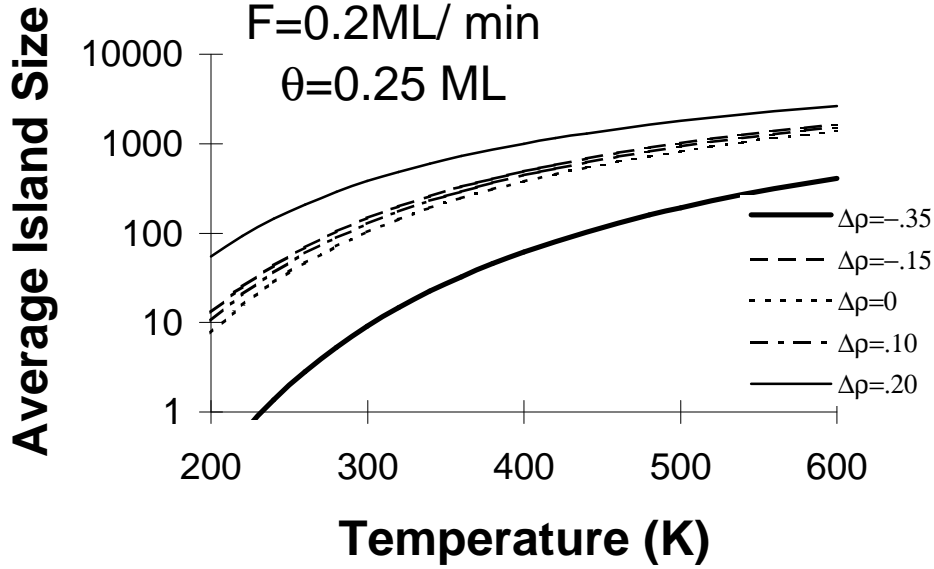


**Figure 2: Ag(100) island sizes using the terrace diffusion barriers of Figure 1.**

where  $\theta$  is the coverage,  $F$  the deposition flux,  $D$  the terrace-diffusion constant (we always assume a generic attempt frequency of  $1 \times 10^{12}$ /sec), and  $a$  the lattice constant. Figure 2 illustrates the temperature dependence of the average island size on Ag(100) for various surface charges under typical electrodeposition conditions. This figure indicates that one can have a large degree of control of the island size during a deposition phase by regulating the electrochemical potential, as a variation of from  $-0.7$  V to  $+0.7$  V relative to the PZC can decrease the average island size from 500 atoms down to 10 atoms. (Such large variations fail to occur on the (111) surface because the variations in  $E_{TD}$  are not so large).

Zhang et al. [23] have quantified the fractal-compact shape transition in terms of a ratio  $t_r/t_a$ , the ratio of residence time an edge atom spends on a given edge of an island to the arrival time of atoms diffusing from the terrace. Regulating this ratio is important in controlling island shapes as  $t_r/t_a < 1$  generally indicates a compact shape. Zhang et al. importantly note that corner as well as edge diffusion determine  $t_r$ , which typically increases the residence time over that from edge diffusion alone.

Figure 3 gives  $t_r/t_a$  as functions of temperature for Ag(100) and Ag(111), respectively. We utilize the expressions of Zhang et al. for  $t_r$  and  $t_a$ , and the SEAM edge and corner diffusion barriers. The deposition flux  $F$  is adjusted to produce a mean island size of 500 atoms for a coverage  $\theta = 0.1$  ML. While all islands on Ag(100) are compact at room temperature (RT), the transition temperature to a fractal shape varies from 130 K to 230 K depending on surface charge. The Ag(111) variations are much more dramatic than for Ag(100) with the opposite sense: The transition temperature varies from 250 K to 960 K with the largest negative surface charge yielding the lowest transition temperature. Though the Ag(111) islands are typically fractal at RT, applying a large enough negative potential ( $\Delta\Phi < -0.5$  V) can produce compact islands instead.

In the late post-deposition phase the islands diffuse and coarsen. The diffusion constant scales according to  $D \sim N^{-\alpha/2}$ , where  $\alpha$  is the scaling exponent. The islands coarsen according to  $\langle N \rangle \sim t^{2\beta}$ , where  $\beta = 1 / (\alpha + 2)$ . Using the expressions of Khare and Einstein [24], which relate cluster diffusion constants with underlying adatom processes, and the SEAM diffusion barriers, we obtain the cluster diffusion constants on Ag(100) depicted in Figure 4. Again, there is a large variation in the magnitude and scaling of the diffusion constant with surface charge. The variation of these quantities with charge reflects the nonmonotonic nature of many of the diffusion constants and the

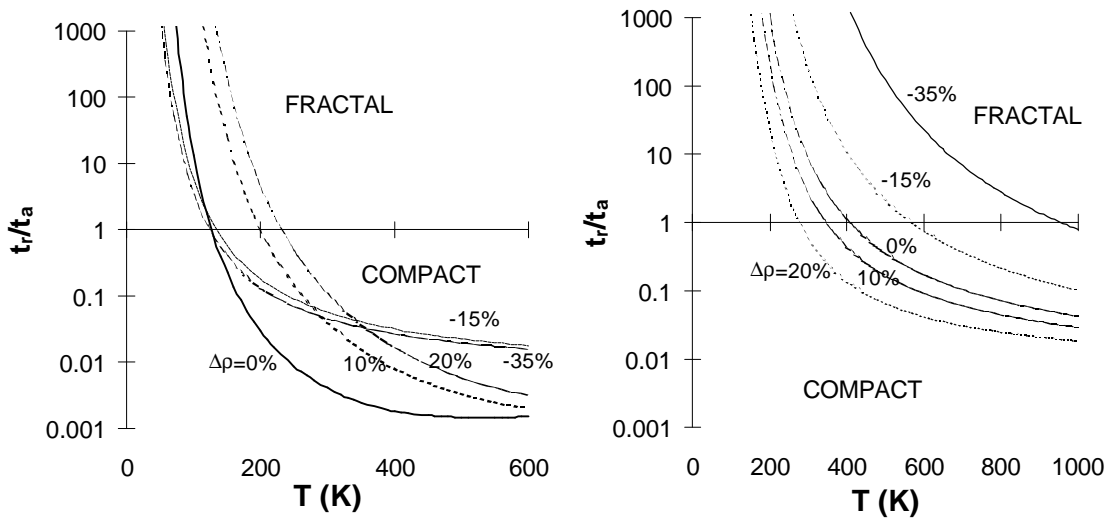


**Figure 3: Ratio of residence time on step-edge to arrival time of atoms from terrace for (a) Ag(100), and (b) Ag(111). The coverage is  $\theta = 0.1$  ML, and the island size is fixed at 500 atoms.**

intricate interplay of these constants in accounting for the cluster diffusion properties. Not only do the magnitudes vary, but so the scaling exponents with evaporation-condensation (for  $\Delta\rho = 20\%$ ),.

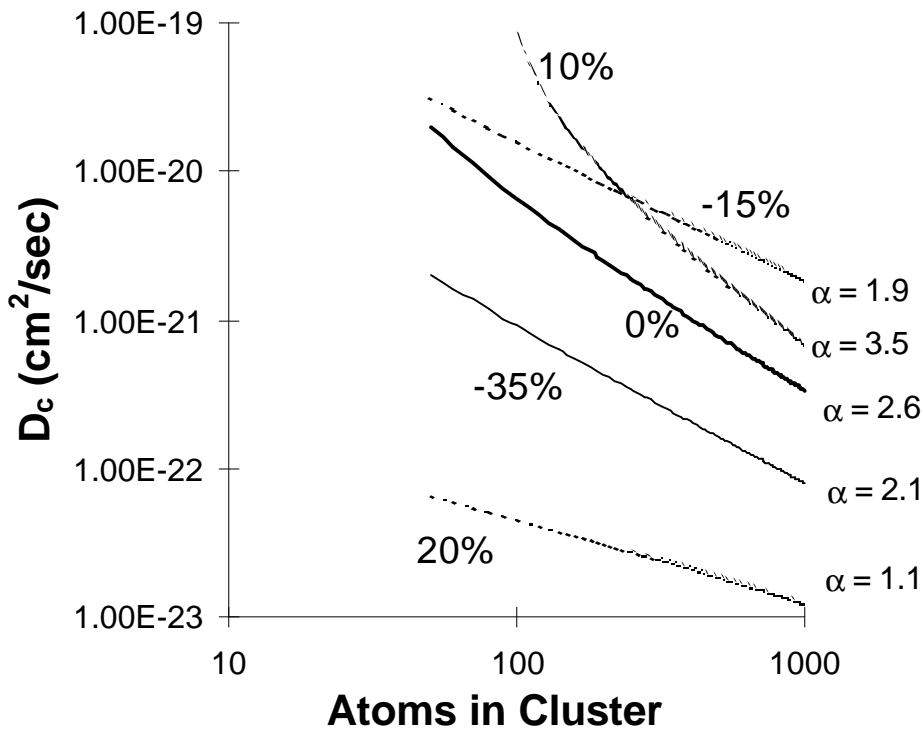


**Figure 4: Cluster diffusion constants at 300 K on Ag(100). The periphery diffusion barrier of ref. [2] determined by the SEAM edge diffusion barrier. The scaling exponent, evaluated near  $N = 300$ , is indicated for each curve.**

terrace diffusion (for  $\Delta p = -15\%$ ,  $-35\%$ ), and periphery diffusion (for  $\Delta p = 0\%$ ,  $10\%$ ) mechanisms all being exhibited. Figure 4 suggests that the electrochemical potential can be used powerfully to control the island coarsening dynamics.

## CONCLUSIONS

Adatom diffusion constants, both on the flat terrace and over or near step-edges, are very sensitive to the surface charge deposited at potentials readily obtainable in electrochemical experiments. This conclusion was reached on the basis of SEAM calculations for Ag(100) and Ag(111) electrodes, but should hold on other metal electrodes as well. The diffusion barriers often exhibit complicated nonmonotonic behavior with the surface charge, with this being the case more so on Ag(100) than on Ag(111). The complicated behavior is a result of the different effects of bond breaking, surface stress, and the transitions between hopping and exchange diffusion as the preferred mechanism. The large variations in diffusion barriers translates into large variations in island size, shape, and island diffusion and coarsening properties. Thus it appears that the electrochemical potential can be used to control these islanding characteristics, both in the deposition and post-deposition phases, to fabricate desired features on the nanoscale. Cycling the potential between deposition and post-deposition phases may even offer a greater degree of control.

Support by The Office of Naval Research and the NSF-MRSEC at the University of Maryland is gratefully acknowledged.

## REFERENCES

- [1] S.G. Corcoran, G.S. Chakarova, and K. Sieradzki, *Phys. Rev. Lett.* **71**, 1585 (1993).
- [2] F.A. Möller, O.M. Magnussen, and R.J. Behm, *Phys. Rev. Lett.* **77**, 3165 (1996).
- [3] C.A. Lucas, N.M. Markovic, and P.N. Ross, *Phys. Rev. Lett.* **77**, 4922 (1996).
- [4] D.M. Kolb, *Prog. in Surf. Sci.* **51**, 109 (1996).
- [5] D.J. Eaglesham and M. Cerullo, *Phys. Rev. Lett.* **64**, 1943 (1990).
- [6] C.L. Fu and K.M. Ho, *Phys. Rev. Lett.* **63**, 1617 (1989).
- [7] K.P. Bohnen and D.M. Kolb, *Surf. Sci.* **407**, L629 (1998).
- [8] M.S. Daw and M.I. Baskes, *Phys. Rev. B* **29**, 6443 (1984).
- [9] J.M. Wen, S.L. Chang, J.W. Burnett, J.W. Evans, and P.A. Thiel, *Phys. Rev. Lett.* **73**, 2591 (1994).
- [10] W.W. Pai, A.K. Swan, Z. Zhang, and J.F. Wendelken, *Phys. Rev. Lett.* **79**, 3210 (1997).
- [11] C.R. Stoldt, C.J. Jenks, P.A. Thiel, A.M. Cadilhe, and J.W. Evans, *J. Chem. Phys.* **111**, 5157 (1999).
- [12] H. Brune, H. Röder, C. Boragno, and K. Kern, *Phys. Rev. Lett.* **73**, 1955 (1994).
- [13] J. Heinonen, I. Koponen, J. Merikoski, and T. Ala-Nissila, *Phys. Rev. Lett.* **82**, 2733 (1999).
- [14] S. Pal and K.A. Fichthorn, *Phys. Rev. B* **60**, 7804 (1999).
- [15] M.I. Haftel and M. Rosen, *Phys. Rev. B* **51**, 4426 (1995).
- [16] M.I. Haftel and M. Rosen, *Surf. Sci.* **407**, 16 (1998).
- [17] M.I. Haftel, M. Rosen, and S.G. Corcoran, *Mat. Res. Soc. Symp.* **451**, 31 (1997).
- [18] Wolfgang Schmickler, *Interfacial Electrochemistry*, Oxford University Press, New York (1996), p26.
- [19] M.I. Haftel and M. Rosen, *Bull. Am. Phys. Soc.* **44**, 1831 (1999).
- [20] A. Hamelin and L. Stoicoviciu, *J. Electroanal. Chem.* **234**, 93 (1987).
- [21] B.D. Yu and M. Scheffler, *Phys. Rev. B* **56**, R15569 (1997).
- [22] J.G. Amar, F. Family, and P.-M. Lam, *Phys. Rev. B* **50**, 8781 (1994).
- [23] T. Zhang, J. Zhong, Z. Zhang, and M.G. Lagally, preprint (1999).
- [24] S.V. Khare and T.L. Einstein, *Phys. Rev. B* **54**, 11752 (1996).